

# THE EFFECT OF CURVATURE ON THE DYNAMIC BEHAVIOUR OF A RAILWAY TRACK

D Kostovasilis The University of Nottingham, University Park, Nottingham, NG7 2RD, UK  
SG Koroma The University of Nottingham, University Park, Nottingham, NG7 2RD, UK  
MFM Hussein The University of Nottingham, University Park, Nottingham, NG7 2RD, UK  
JS Owen The University of Nottingham, University Park, Nottingham, NG7 2RD, UK

## 1 INTRODUCTION

Noise and vibration from moving trains are important environmental issues affecting residents near railway lines. Modelling the dynamic behaviour of tracks is important to develop a good understanding about the physics which is essential to providing solutions. A large number of models have been reported in the literature on the dynamic behaviour of railway tracks. Most of these focus on straight tracks with less attention paid to curved tracks. This is mainly attributed to the higher complexity associated with modelling of curved tracks compared to straight ones. However, curved tracks are reported to have additional problems which increase the need for further research.

In the literature, the effect of curvature of beams has been subjected to limited study. Yang et al. (2001)<sup>2</sup> derived the analytical solution for the dynamic response of a horizontally curved beam subjected to vertical and horizontal moving loads. This was solved for a simply supported beam and accounting for the first mode of vibration only. Wu and Chiang (2003)<sup>3</sup> developed a new approach to analyse the out-of-plane vibration of circular arches due to moving loads using curved beam elements. A detailed review is also provided with regard to the out-of-plane vibration of curved beams subjected to moving loads for both analytical and numerical approaches. More recent approaches include that of Ang and Dai (2012)<sup>4</sup> who used the moving element method to model a curved beam subjected to a moving load using straight beam elements. Calim (2012)<sup>5</sup> studied the forced vibration of curved beams on two-parameter elastic foundation subjected to impulse loading. None of the literature cited above analysed curved beams under harmonic loads.

In this paper a curved track is formulated as a beam on elastic foundation and is analysed using a matrix approach. The model is discretised using straight beam elements which are formulated as Euler-Bernoulli beams. Torsional effects are also taken into account. The paper presents results describing the dynamics of a curved track with focus on forces transmitted to the track bed. Calculations are performed for harmonic moving loads and the track-bed forces are compared against those for straight tracks. The effects of curvature and loads frequency are also investigated.

## 2 FORMULATION OF THE MODEL

### 2.1 Description of the Load

In this study a moving harmonic load as shown in Fig.1 is considered, in the following form:

$$F_{ap} = A \cos(\bar{\omega}t + \phi) \quad (\text{Eq. 1})$$

where  $A$  is the amplitude,  $\bar{\omega}$  is the frequency of the harmonic load,  $t$  denotes time and  $\phi$  is an initial phase to ensure that the load arrives at the mid-span with maximum amplitude for all frequencies. The load is applied vertically and moves with speed  $V$  along the centreline of the beam.

## 2.2 Track Model

Two models were developed for this paper, a straight track and a curved track model. Both models are discretely supported through rail-pads on a two-parameter visco-elastic foundation with pad-stiffness  $k_p$  (N/m) and damping  $c$  (Ns/m). This is done through using a spring and a dashpot in parallel, also known as the Kelvin-Voigt model. The damping is applied as a percentage ( $\zeta$ ) of the critical damping ( $c_{cr}$ ) of the system,  $c = \zeta c_{cr}$ . The supports are repeated at a fixed distance  $L$  (m). The foundation itself rests on a rigid base. The total length of both tracks is denoted  $L_t$  (m) with a total number of spans  $n_t = L_t/L$ . The curved track is also defined by its radius of curvature,  $R$ . Thus the total angle ( $\theta$ ) for the curved track is:

$$\theta = L_t / R \quad (\text{Eq. 2})$$

Figures 1a and 1b show the track models, with their local and global Cartesian co-ordinate axes.

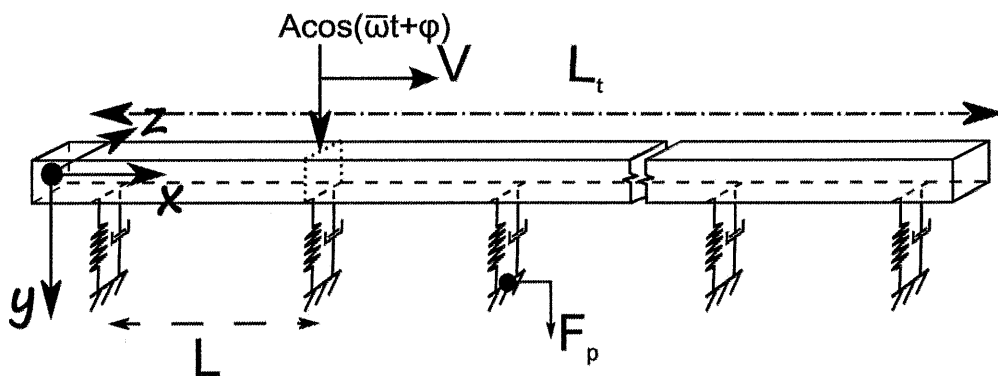


Figure 1a: Layout of the straight track models

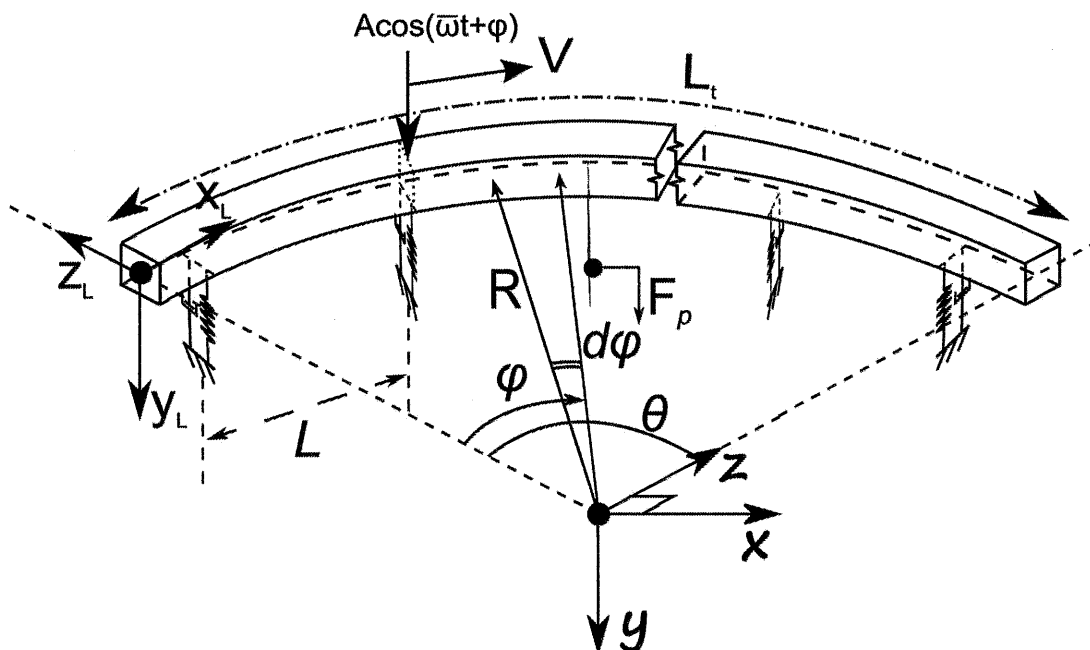


Figure 1b: Layout of the curved track models

## 2.3 Discretisation of the Model

In this paper, for both models the beam elements between the supports have been discretised into a finite number of elements,  $n$  with each element having a length  $L_{el} = L/n$ . In the curved beam model straight elements are used between nodal points. The stiffness and damping of the pads are applied at the end nodes of each beam element every  $n$  nodes.

### 2.3.1 Global Mass ( $\mathbf{M}_G$ ) and Stiffness ( $\mathbf{K}_G$ ) Matrices

Each node has six degrees of freedom (dof's) accounting for displacements and rotations in the vertical horizontal and axial direction. Each individual element is modeled using straight Euler-Bernoulli beam elements for both models. The stiffness and mass matrices for the elements are presented in the literature<sup>6,8</sup>. These have also been used in this work.

For the straight track model, since the local co-ordinate axes coincide with the global co-ordinate axis, the assembling of the global mass and stiffness matrix is a straight forward process. For the curved beam model though, the element matrices need to be converted from their local co-ordinates ( $\mathbf{M}_L, \mathbf{K}_L$ ) to the global co-ordinates ( $\mathbf{M}_G, \mathbf{K}_G$ ) before they are entered in the global matrices. This is achieved by using the transfer matrix  $\mathbf{T}$  as follows:

$$\mathbf{M}_G = \mathbf{T}^T \mathbf{M}_L \mathbf{T} \text{ and } \mathbf{K}_G = \mathbf{T}^T \mathbf{K}_L \mathbf{T} \quad (\text{Eq. 3, 4})$$

where the superscript ' $T$ ' denotes the transpose of the matrix. The transfer matrix is calculated as:

$$\mathbf{T} = \begin{bmatrix} \mathbf{D} & 0 & 0 & 0 \\ 0 & \mathbf{D} & 0 & 0 \\ 0 & 0 & \mathbf{D} & 0 \\ 0 & 0 & 0 & \mathbf{D} \end{bmatrix} \text{ where } \mathbf{D} = \begin{bmatrix} \cos(\theta_{el}) & 0 & \sin(\theta_{el}) \\ 0 & 1 & 0 \\ -\sin(\theta_{el}) & 0 & \cos(\theta_{el}) \end{bmatrix} \quad (\text{Eq. 5, 6})$$

It is noted here, that  $\theta_{el}$  denotes the angle between the element local x-axis and the global x-axis. After the transformation of the stiffness matrix, the pad stiffness will be added to the relevant degrees of freedom and a damping matrix of the same size will be created to account for the pad damping.

### 2.3.2 Position of the Load and Shape Functions

While the load moves within an element over time, its position does not always coincide with that of a node. For those intermediate positions, the concentrated force is approximated by converting it to equivalent end-node loads and moments, for the two nodes enclosing that position. This approximation is achieved by using the shape function vector  $\mathbf{N}$ .  $\mathbf{N}$  is a scalar with size equal to the degrees of freedom of the whole system, having all entries equal to zero apart from those regarding the vertical displacement and bending of the two nodes of interest. These entries are evaluated from the following<sup>1</sup>:

$$\begin{aligned} \text{Left-node} \quad N_{L_{vd}} &= 1 - 3\left(\frac{x_{el}}{L_{el}}\right)^2 + 2\left(\frac{x_{el}}{L_{el}}\right)^3 & N_{L_{rot}} &= x_{el}\left(\frac{x_{el}}{L_{el}} - 1\right)^2 \\ \text{Right-Node} \quad N_{R_{vd}} &= 3\left(\frac{x_{el}}{L_{el}}\right)^2 - 2\left(\frac{x_{el}}{L_{el}}\right)^3 & N_{R_{rot}} &= x_{el}\left(\left(\frac{x_{el}}{L_{el}}\right)^2 - \frac{x_{el}}{L_{el}}\right) \end{aligned} \quad (\text{Eq. 7})$$

where  $x_{el} \in [0, L_{el})$  is the position of the load from the left node. Finally the force vector for the whole system is computed from Equation 8 as:

$$\mathbf{F} = \mathbf{N}\mathbf{F}_{ap} \quad (\text{Eq. 8})$$

## 2.4 Equations of Motion and System Response

The classical equation of motion to describe the above system is:

$$\mathbf{M}_G \ddot{\mathbf{u}} + \mathbf{C}_G \dot{\mathbf{u}} + \mathbf{K}_G \mathbf{u} = \mathbf{F} \quad (\text{Eq. 9})$$

This equation is solved numerically using a composite implicit time integration scheme which has been presented in detail by Bathe and Baig (2005)<sup>9</sup>. In this scheme the solution is first estimated for the sub-step  $t+\gamma\Delta t$  using the trapezoidal rule with the following expressions for the velocity and acceleration:

$$\dot{\mathbf{u}}_{t+\gamma\Delta t} = \alpha(\mathbf{u}_{t+\gamma\Delta t} - \mathbf{u}_t) - \dot{\mathbf{u}}_t \quad (\text{Eq. 10})$$

$$\ddot{\mathbf{u}}_{t+\gamma\Delta t} = \alpha^2(\mathbf{u}_{t+\gamma\Delta t} - \mathbf{u}_t - \dot{\mathbf{u}}_t \gamma \Delta t) - \ddot{\mathbf{u}}_t \quad (\text{Eq. 11})$$

with  $\alpha = 2/\gamma\Delta t$  and  $\gamma = 1/2$ . At  $t = 0$  it is assumed that the system is at rest with initial displacement and velocity equal to zero and acceleration:

$$\ddot{\mathbf{u}}_{t=0} = [\mathbf{M}_G]^{-1} \mathbf{F}_{t=0} \quad (\text{Eq. 12})$$

Using Equations 9-12 the response of the system at time  $t+\gamma\Delta t$  is:

$$\mathbf{u}_{t+\gamma\Delta t} = \mathbf{H}^{-1}(\mathbf{F}_{t+\gamma\Delta t} + (\mathbf{M}_G \alpha^2 + \mathbf{C}_G \alpha) \mathbf{u}_t + (2\mathbf{M}_G \alpha + \mathbf{C}_G) \dot{\mathbf{u}}_t + \mathbf{M}_G \ddot{\mathbf{u}}_t) \quad (\text{Eq. 13})$$

where

$$\mathbf{H} = \mathbf{M}_G \alpha^2 + \mathbf{C}_G \alpha + \mathbf{K}_G \quad (\text{Eq. 14})$$

Then the velocity and acceleration are calculated using Equations 10 and 11. In order to progress the solution for time  $t+\Delta t$  the derivative of  $\mathbf{u}_{t+\Delta t}$  is written in terms of the values  $\mathbf{u}_t$ ,  $\mathbf{u}_{t+\gamma\Delta t}$  and  $\mathbf{u}_{t+\Delta t}$  as:

$$\dot{\mathbf{u}}_{t+\Delta t} = c_1 \mathbf{u}_t + c_2 \mathbf{u}_{t+\gamma\Delta t} + c_3 \mathbf{u}_{t+\Delta t} \quad (\text{Eq. 15})$$

where

$$c_1 = \frac{1-\gamma}{\gamma\Delta t} \quad c_2 = \frac{-1}{(1-\gamma)\gamma\Delta t} \quad \text{and} \quad c_3 = \frac{(2-\gamma)}{(1-\gamma)\Delta t} \quad (\text{Eq. 16})$$

Similarly:

$$\ddot{\mathbf{u}}_{t+\Delta t} = c_4 \dot{\mathbf{u}}_t + c_5 \dot{\mathbf{u}}_{t+\gamma\Delta t} + c_6 \dot{\mathbf{u}}_{t+\Delta t} \quad (\text{Eq. 17})$$

Substituting Equation 15 and 17 back to Equation 9 we get:

$$\mathbf{u}_{t+\Delta t} = \mathbf{J}^{-1}(\mathbf{F}_{t+\Delta t} - (c_1 c_3 \mathbf{M}_G + c_1 \mathbf{C}_G) \mathbf{u}_t - (c_2 c_3 \mathbf{M}_G + c_2 \mathbf{C}_G) \mathbf{u}_{t+\gamma\Delta t} - c_1 \mathbf{M}_G \dot{\mathbf{u}}_t - c_2 \mathbf{M}_G \dot{\mathbf{u}}_{t+\gamma\Delta t}) \quad (\text{Eq. 18})$$

where

$$\mathbf{J} = c_3^2 \mathbf{M}_G + c_3 \mathbf{C}_G + \mathbf{K}_G \quad (\text{Eq. 19})$$

and the solutions at time  $t+\gamma\Delta t$  have already been calculated.

## 2.5 Force transmitted on the foundation

After deriving the displacement and velocity vectors for the vertical degree of freedom at each time-step for the beam, the vertical force transmitted to the foundation can be written as:

$$\mathbf{F}_p = k_p \mathbf{u}_y + c_p \dot{\mathbf{u}}_y \quad (\text{Eq. 20})$$

## 3 RESULTS AND DISCUSSION

For the calculations the following rail, track and foundation parameters were used: Young's modulus  $E = 210 \times 10^9 \text{ N/m}^2$ , second moment of area around z-axis  $I_z = 3038.3 \times 10^{-8} \text{ m}^4$ , second moment of area around y-axis  $I_y = 512.3 \times 10^{-8} \text{ m}^4$ , polar moment of inertia  $J = I_z + I_y$ , rail cross-sectional area  $A = 7.672 \times 10^{-3} \text{ m}^2$ , rail mass  $m = 60.21 \text{ kg/m}$ , rail foot width  $b = 150 \text{ mm}$ , shear modulus  $G = 79.56 \times 10^9$ , total track length  $L_t = 36 \text{ m}$ , support distance  $L = 0.6 \text{ m}$ , number of elements  $n = 2$ , foundation damping ratio  $\zeta = 0.1$  (10%) and pad stiffness  $k_p = 20 \times 10^6 \text{ N/m}$ . The time step  $\Delta t$  is evaluated based on the frequency. In order to satisfy the Nyquist criterion, the minimum permissible time step needs to be at least half the reciprocal of the excitation frequency. For the following calculations  $\Delta t$  is taken to be at least five times smaller than  $\Delta t_{\min}$ . The total number of degrees of freedom is 726. Additional stiffness (+99 $k_p$ ) and damping (+9 $c_p$ ) have been added to the first and last node to act as absorbing boundaries.

For radius variation between 50 and 350 m and arc length of 0.3 meters, approximating the length of the straight element by that of the arc length, results in an error of less than 0.1%. Also the length of the track considered has been found to be sufficient, in order for the boundary effects to be negligible in the frequency range investigated in this paper.

Following are the results investigating the effect of frequency and radius, on the forces transmitted from the rail pad to the foundation at the mid-span of the straight track and the versine of the curved track ( $x_{\text{pad}} = L_t/2$  from the origin). It should be noted that all results have been normalised with respect to the input force for the above system properties.

In Figure 2 the maximum force transmitted to the foundation at the mid-span has been plotted against frequency for a speed of (a) 20 m/s on the left and (b) 60 m/s on the right. This has been done for the straight track and two curved tracks with radii of 350m and 50m. The results for all three tracks are almost identical. At both speeds, the peak force occurs near the cut-on frequency  $f_{co} = \sqrt{k/m}$ . It is observed that for the current system variables for frequencies near the cut-on frequency, the maximum force is higher for a load with velocity 20 m/s than that at with 60 m/s.

When considering vertical forces for the straight track, the force at a point in any element are transmitted as shear forces and bending moments from that element to the adjacent at the positions of the end nodes. For the case of the curved track the same happens for the shear forces, but not the bending moments. Since the elements are at an angle, the bending moments of one element are transferred as both bending and twisting moments for the next element. This creates torsional forces in the beam which in turn affect the forces transmitted to the foundation. The reason why the responses for the straight and curved track are so similar can be explained from the fact that the angles between the elements are very small.

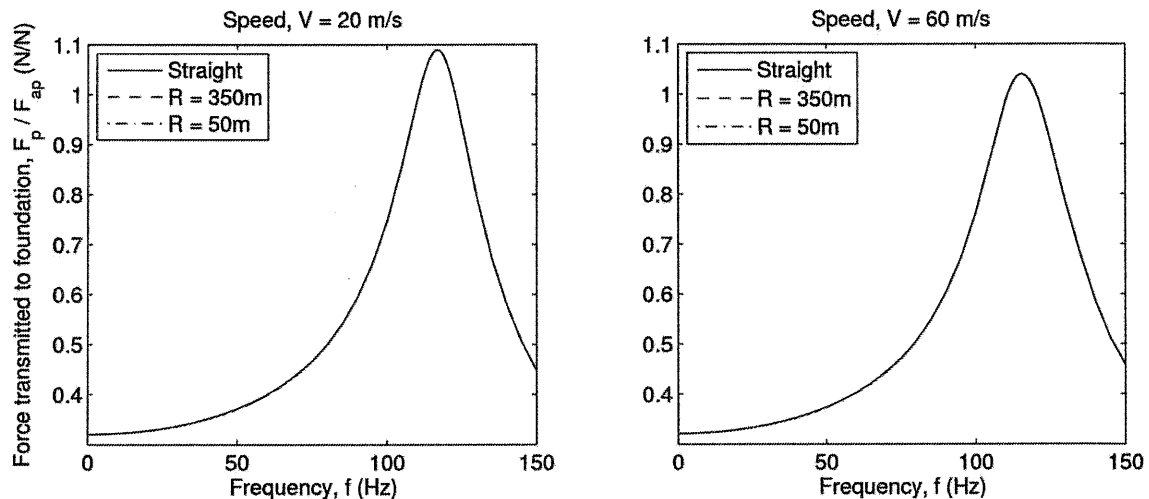


Figure 2: Frequency response of force transmitted to the foundation for straight and curved tracks for a load with velocity a) 20m/s and b) 60 m/s

## 4 CONCLUSION AND FUTURE WORK

In this paper we have investigated the effect of curvature on the vertical forces transmitted to the foundation due to a vertical harmonic moving load. The effect of frequency of the load was also considered. Further research is on-going to improve the current model of the curved track. Plans for continuing this work comprise:

- Use of curved elements instead of straight
- Account for horizontal forces
- Investigate the effect of torsion

## 5 REFERENCES

1. J.R. Rieker, Y.H. Lin and M.W. Trethewey, 'Discretization considerations in moving load finite element beam models', *Journal of Finite Elements in Analysis and Design*, Vol. 21, 129-144. (1996).
2. Y.B. Yang, C.M. Wu and J.D. Yau, 'Dynamic response of a horizontally curved beam subjected to vertical and horizontal moving loads', *Journal of Sound and Vibration*, Vol. 242, Iss. 3, 519-537. (2001)
3. J.S. Wu and L.K. Chiang, 'Out-of-plane responses of a circular curved Timoshenko beam due to a moving load', *International Journal of Solids and Structures*, Vol. 40, 7425-7448. (2003)
4. K.K. Ang and J. Dai, 'Response analysis of high speed train travelling on curved track', *Proceedings of the 14<sup>th</sup> International Conference on Computing in Civil and Building Engineering (ICCCBE)*, Moscow (2012)
5. F.F. Calim, 'Forced vibration of curved beams on two-parameter elastic foundation', *Journal of Applied Mathematical Modelling*. Vol. 36, 964-973. (2012)
6. JS Przemieniecki, *Theory of Matrix Structural Analysis*. McGraw-Hill, New York (1968)
7. K.J. Bathe, 'Finite element procedures', Vol. 2. No. 3. Englewood Cliffs: Prentice hall. (1996)
8. W.D. Pilkey, 'Analysis and design of elastic beams: Computational methods'. Wiley. (2002)
9. K.J. Bathe and M.M.I. Baig, 'On a composite implicit time integration procedure for nonlinear dynamics'. *Journal of Sound and Vibration*, Vol. 85, 2513-2524. (2005)